Available online at www.sciencedirect.com
ScienceDirect
Optik 118 (2007) 221–231
Optik Optics
www.elsevier.de/ijleo

Application of picosecond optical guiding-center solitons in single-mode fibers to precise synchronization of a radio-interferometer

Alexandre S. Shcherbakov[a,*], Alexey Yu. Kosarsky[b], Mauro Sanchez Sanchez[a], Vladimir N. Zvegintsev[c]

[a]*Department of Optics, National Institute for Astrophysics, Optics & Electronics, A.P. 51 y 216, Puebla, Pue., 72000, Mexico*
[b]*LLC "Petro", Peterhoff Chausse 71, St. Petersburg, 198206, Russian Federation*
[c]*"Vector" Research Institute, Federal State Unitary Enterprise, 197276, St. Petersburg, Russian Federation*

Received 1 December 2005; accepted 3 March 2006

Abstract

Picosecond optical guiding-center solitons of the first order, peculiar for the cubic Ginzburg–Landau systems, are considered as the sync-signal carriers, being attractive for the transmission through optical fiber network. At first, we analyze the model, governed by the complex cubic Ginzburg–Landau equation in a reduced form, and present an approximate analytical description for the evolution of the main parameters inherent in guiding-center solitons. Then, these soliton-like pulses are compared with fundamental solitons adiabatically perturbed by low losses in optical fiber, being also potentially suitable to be the sync-signal carriers. This comparison suggests a conclusion that guiding-center solitons have considerable advantages in applying as lock-on signals from the viewpoints of energy consumption and ease of implementation. Interferometric technique of measuring time intervals with the help of train-average field strength correlation functions to a sub-picosecond accuracy is developed in the event of arriving the optical soliton-like pulses at a high repetition rate. Such an advantage of this technique as the ability of operating on the trains of low-power picosecond optical pulses, in particular, guiding-center solitons in single-mode fibers is revealed. Results of trial experiments with the mock-up, implemented as optical part of the sync-network for a short base radio-interferometer, are presented.

Keywords: Guiding-center soliton; Sync-network; Interferometric technique

1. Introduction

At present, the majority of data processing systems uses the lock-on signals, since the asynchronous systems as well as the self-timed data-flow networks have not been adequately developed. Naturally, the delta-function pulse is an ideal lock-on signal, but in practice, it can be realized only approximately. That is why general requirements to the lock-on signals have to be satisfied in the synchronously processing system with an arbitrary arrangement. These signals should be precisely determined in the time scale compared with a temporal interval, corresponding to the cutoff frequency in data flow, or to the jitter time conditioned by any internal instabilities or external perturbations. In digital processors, the sync-signals should be much shorter than the time peculiar to the simplest logic operation or than the repetition period for such operations. Consequently, the requirements to both the duration and the repetition period of lock-on signals increase by growth of the informative capacity, speed of operation, or processing accuracy in a system. In recent

*Corresponding author.
E-mail address: aiex@inaoep.mx (A.S. Shcherbakov).

0030-4026/$ - see front matter © 2006 Elsevier GmbH. All rights reserved.
doi:10.1016/j.ijleo.2006.03.015

years, aforementioned problems had been extended to optics due to the progress in optical information technologies. Certain of these problems may be resolved by looking at the technique based on the application of ultrashort optical pulses, which are able to play the part of delta-function like pulses under certain conditions. Therefore, we consider some aspects of implementing an all-optical sync-network using ultrashort optical pulses as the lock-on signal carriers. Various approaches can be applied to establish the clock time in synchronously processing system. For instance, in a lengthy-span optical fiber transmission system with the pulse-code modulation, the lock-on signals, which are impressed onto binary format on the transmitter end, are recovered on the receiver end by extracting the clock frequency. On the contrary, a special purpose sync-network is usually included into the digital data processing system. Bearing the implementation of just optical processing system in mind, one ought to set aside the simplest case when identical optical lock-on signals are one-directionally distributed from the source all over the processing system, and this source represents a separate unit. Evidently, to pass optical lock-on signals with a minimal pulse width at a maximal repetition frequency and to distribute them all over the system without any revisions in the architecture of processing systems the fiber technique is the most promising. In order to make the best use of a modern fiber technique, the preference should be given to the lock-on signals in the form of picosecond solitons being capable of passing through single-mode low-loss fibers at the repetition rate up to 10^{11} Hz. As this takes place, the accuracy of the synchronization is ultimately restricted by an error in determining the energetic center of a sync-pulse. Such an error is no more than the sync-pulse width, so the application of soliton regime to transmitting the lock-on signals through single-mode fibers is an essential prerequisite to create the processing system with a picosecond accuracy of synchronization. Naturally, with the use of solitons in a fiber, the precision of synchronization will be increased resulting in a subject of much current interest in connection with operating a modern radio-interferometer, whose angular resolution should be high enough, but the base has to be short.

For the first time, the guiding-center solitons were studied theoretically by Hasegawa and Kodama [1–3] as well as by Blow and Doran [4]. They considered that the behavior of pulses is analogous to the motion of a charged particle in an inhomogeneous magnetic field, where even if the instantaneous position of the particle oscillates rapidly at the gyrofrequency, the center of the oscillatory motion, called the guiding center, moves smoothly. Such an analogy led to a new theory of pulse propagation in the presence of periodic perturbations with a period much shorter than the dispersion distance. Originally, the area of existence for such solitary waves was estimated by the condition $\Gamma \gg 1$, where Γ is the ratio of the dispersion distance to the loss distance. Then, Shcherbakov et al. [5–7] discovered and investigated, both theoretically and experimentally, that originating and developing the guiding-center solitons is possible when $\Gamma \geqslant 1$. Later on, Shcherbakov and Kosarsky [8,9] used a specially developed technique of computer simulation to classify areas of shaping bright solitary waves of the first order in systems of the complex cubic Ginzburg–Landau equation and to demonstrate it amply clear that the area of existence for picosecond guiding-center solitons in single-mode fibers can be enlarged in the region $\Gamma < 1$. The intention of exploiting picosecond guiding-center solitons in an effort of synchronization had required impressive additional analyses. In response to that, approximate analytical description of the main parameters, reflecting the evolutions of the guiding-center solitons of the first order, has been developed in the paper presented. Keeping in hands similar results, it was necessary to select the best-suited carrier for sync-signals. For this purpose, two types of optical solitary waves, namely, fundamental optical solitons adiabatically perturbed by losses and guiding-center solitons, which both can be potentially exploited as the signal carriers in a fiber network for synchronization, are compared with each other from the viewpoint of the energy consumption. It is shown that the guiding-center soliton offers the advantage of less energetic sync-signal carrier over another soliton-like pulses. In addition, it turns out easily to generate sync-signals in the form of guiding-center solitons, all other factors being equal, for instance, the accuracy of synchronization, because they are considerably wider initially.

In Section 2, the problem of precise synchronization for a short base radio-interferometer with the sync-network, based on picosecond optical solitons in single-mode fibers, is considered. Section 3 is concerned with the theoretical description of developing the guiding-center solitons in low-loss single-mode fibers. Section 4 is devoted to comparison guiding-center solitons with fundamental optical solitons in fibers from the viewpoint of transmitting the sync-signals. Features inherent in the chosen optical interferometric technique of measuring the temporal intervals are analyzed in Section 5. Both the schematic arrangement and the results, obtained during the trial experiments with a specially created mock-up representing an optical part of the sync-network for a radio-interferometer, are presented in Section 6. Section 7 lists a few conclusive remarks.

2. General consideration of the problem

Let us consider the concrete scheme for a precise synchronization of a two-antenna short base radio-interferometer, which consists of two observing posts and the central processing unit, see Fig. 1. The problems of establishing the clock time in a system and determining

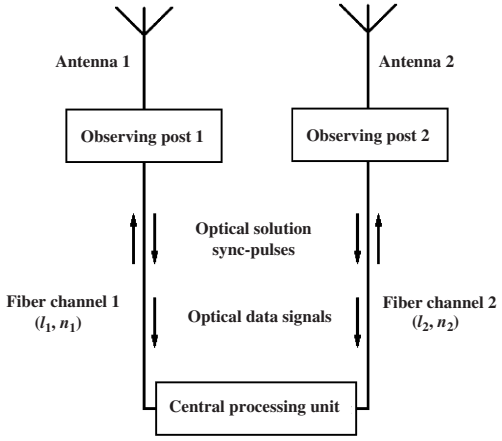

Fig. 1. General scheme of a precise synchronization for a two-antenna radio-interferometer.

the clock skew between two posts may be reduced to the precise collation of local time scales using the lock-on signals. For example, from the standpoint of radio-astronomy, the key value under observation therewith is the geometric time-delay $t_1 = c^{-1}\ L \cdot \sin\theta$, where c is the light velocity, θ is the angle of wave front arrival, L is the base length.

To calculate the geometric time-delay, being in a state of constant flux, the data about some wave front, scanning the observing posts, should be transmitted to the central processing unit. The data signals are passed by two different channels and, consequently, the temporal mismatch of data signals in these channels t contains: the geometric time-delay t_1, the difference $t_2 = c^{-1}(l_1 n_1 - l_2 n_2)$ in the traveling time (here $l_{1,2}$ and $n_{1,2}$ are the geometric lengths and refractive indexes of transmitting fiber channels), and an occasional time-delay t_3 conditioned by external perturbations, so we get

$$t = t_1 + t_2 + t_3. \tag{2.1}$$

The lock-on signals are generated by the central processing unit and then they are concurrently directed to either observing post by different channels, being just those channels, which are used for the transmission of data signals. Later, after a passage over the observing posts, these lock-on signals come back at the central processing unit. The clock skew between the energetic centers of channel passed sync-pulses is given by $t_C = 2(t_2 + t_3)$. Thus, the magnitude of t_C could be used to find the geometric time-delay $t_1 = t - t_C/2$. Such a solution of the sync-problem is rather steady in relation to casual perturbations having influence over the magnitude of t_3. The sync-accuracy is determined by the accuracy of measuring the clock skew between the energetic centers of sync-pulses and also by originating casual variations in the shape, spectrum and group velocity of pulses in both the transmitting channels. Fortunately, just fundamental solitons inherent in Ginzburg–Landau systems are the most tolerant to variations of this kind, because temporal locations of their energetic centers are practically insensitive to similar perturbations of pulses. The principal measurable value is the clock skew t_C between the energetic centers of ultrashort optical sync-pulses passed in parallel through two different fiber channels. Initially, one ultrashort optical pulse is injected into two channels – just two fibers, and then the soliton signals arrive at the ports of registration after the times τ_1 and τ_2, respectively, given by

$$\tau_{1,2} = c^{-1}\ l_{1,2}\ n_{1,2} + \delta\ t_{1,2}, \tag{2.2}$$

where $\delta t_{1,2}$ are the time-delays conditioned by external perturbations. The clock skew between these pulses can be written as

$$t_C = \tau_1 - \tau_2 = c^{-1}(l_1 n_1 - l_2 n_2) + \delta\ t_1 - \delta\ t_2. \tag{2.3}$$

In this scheme, the clock skew appears as a temporal shift between two picosecond optical pulses corresponding to a common initial optical pulse, so that pulse stirring is not available. However, this brings up the problem of supervising, that is to say, estimating the clock skew between the energetic centers of sync-pulses with a picosecond accuracy, suggesting that one is in need of accomplishing the photon-to-electron conversion with the time constant lying in a sub-picosecond range. Nevertheless, this difficulty can be successfully get over if the lock-on signal source generates an uninterrupted train of picosecond optical pulses at a sufficiently high repetition rate. To keep picosecond accuracy the train-average clock skew can be measured as a temporal shift between two pulse trains via shaping all-optically the second-order correlation function of these trains. The optical scheme, measuring the train-average clock skew, as a whole represents an all-fiber Mach-Zehnder interferometer, and the performances of this scheme are conditioned by the properties of such an interferometer. The proper train-average clock skew between pulse trains passing through two parallel channels, one of which contains the tunable time-delay under control, is measured by two beam sliding Michelson interferometer. With a high repetition rate of sync-pulses the use of sliding interferometer provides the procedure of sampling to form the cross-correlation function all-optically and to maintain an exactly scaled conversion from the analysis of ultrafast phenomena at optical frequencies to the analysis of these processes with a speed of operation being accessible for electronics. Just temporal sliding in the Michelson interferometer realizes an all-optical sampling procedure in detecting the correlation function in such a way that all the further processing can be made electronically. Generally, to detect the correlation function at a sub-picosecond time resolution both the nonlinear second harmonic generation technique and the proper interferometric one are successfully used. With the nonlinear technique, when the response time of nonlinear crystal is less than 10 fs, the

photodetector integrates the signal being linearly proportional to the intensity of the second harmonic light wave, so any information about the phase of light wave is fallen. However, the efficiency of the second harmonic generation is too small at low level of pulses generated by such sources as, for example, mode-locked semiconductor lasers, hindering the processing of correlation function and sending us in search of the other way. Consequently, it is expedient to look at the proper interferometric technique, which is suited to processing the pulse signals accessible for semiconductor laser sources. At the same time, the interferometric technique is sensitive to the phase characteristics of light wave, in particular to its time coherence. The uniqueness in the results of measurements can be achieved only if the detected light represents a faint background together with a train of transform-limited pulses with a smooth envelope. Such is indeed the case when the picosecond optical solitons in single-mode fibers can be successfully used as the lock-on signals.

3. Developing bright picosecond guiding-center solitons in optical fiber

Evolution of bright solitary waves in the media with a weakly focusing cubic-law nonlinearity, anomalous dispersion of the group velocity, and the losses γ is described by the complex cubic Ginzburg–Landau equation in a reduced form [10,11]

$$\mathrm{i}\frac{\partial A}{\partial z}-\frac{1}{2}\frac{\partial^2 A}{\partial \tau^2}-|A|^2A+i\Gamma A=0. \tag{3.1}$$

Here A is the field amplitude normalized to the amplitude of a fundamental soliton in the case of $\gamma=0$. The normalized independent variables z and τ are connected with the propagation distance x and the retarded time t in tracking coordinate system as $z=xZ_{\mathrm{D}}^{-1}$ and $\tau=t\tau_0^{-1}$; where $Z_{\mathrm{D}}=\tau_0^2|k_2|$ is the dispersion distance, k_2 is the dispersion coefficient ($k_2<0$ in the anomalous dispersion region), and τ_0 is the initial width of solitary wave, determined by the level of $\mathrm{sech}1=0.65$. Because of the losses, the dynamics of developing the bright pulse is conditioned by the factor $\Gamma=\gamma Z_{\mathrm{D}}$. The reduction of the complex cubic Ginzburg–Landau equation to Eq. (3.1) lies in the fact that both the spectral filtering and the nonlinear absorption processes are neglected, so the coefficients in the second and third terms are real-valued in Eq. (3.1). We assume that initially the solitary waves do not have the frequency chirp b and satisfy the following boundary conditions

$$A(z=0,\tau)=a_0\mathrm{sech}(\tau)\quad b(z=0,\tau)=0. \tag{3.2}$$

Here the normalized initial amplitude a_0 determines an initial excess of the pulse amplitude over the magnitude of A_0 for corresponding fundamental soliton. Having in mind the only solitary waves of the first order, we restrict ourselves to considering the interval $1.0\le a_0\le 1.5$ [12].

We take the project of solution to Eq. (3.1) as a product $A(z,\tau)=h(z,\tau)Q(z,\tau)$, where $h(z)=a_0\exp(-\Gamma z)$ and $a_0=h(z=0)$. In so doing, the complex function $Q(z,\tau)$ has to satisfy the following partial differential equation

$$i\frac{\partial Q}{\partial z}-\frac{1}{2}\frac{\partial^2 Q}{\partial \tau^2}-h^2(z)\left|Q\right|^2Q=0. \tag{3.3}$$

The constant a_0 is taken so that the condition $Z_A^{-1}\int_0^{Z_A}h^2(z)\,\mathrm{d}z=1$ is true along distances $z\le Z_A$ [1] and, consequently, $a_0^2=2\Gamma Z_A[1-\exp(-2\Gamma Z_A)]^{-1}$, and $a_0\ge 1$. Then, we will search a solution $Q(z,\tau)$ to Eq. (3.3) as the sum of two quadrature components $Q(z,\tau)=[q(z,\tau)+\mathrm{i}p(z,\tau)]\exp[\mathrm{i}\varphi(z,\tau)]$, whereas the first component, namely, $q(z,\tau)\exp[\mathrm{i}\varphi(z,\tau)]$ will be chosen in the form of one-soliton solution to the cubic Schrödinger equation [3,11]

$$q(z,\tau)\exp[\mathrm{i}\varphi(z,\tau)]=\eta\sec h[\eta(\tau-\kappa z)]\times\exp\left[-\mathrm{i}\kappa\tau-\frac{\mathrm{i}z}{2}\left(\eta^2-\kappa^2\right)\right]. \tag{3.4}$$

Here, η determines both the amplitude and the width for fundamental soliton, k describes the frequency shift. The first component, expressed by Eq. (3.4), represents the guiding center of a pulse. The second component may be taken in the form $p(z,\tau)\approx R_0(z)q^3(z,\tau)$, with the function

$$R_0(z)=z+a_0^2(2\Gamma)^{-1}[\exp(-2\Gamma z)-1], \tag{3.5}$$

satisfying the condition $Z_A^{-1}\int_0^{Z_A}R_0(z)\,\mathrm{d}z=0$. Thus, the complex amplitude of solitary pulse can be expressed as

$$A(z,\tau)=a_0\exp(-\Gamma z)q(z,\tau)\times\left[1+\mathrm{i}R_0(z)q^2(z,\tau)\right]\exp[\mathrm{i}\varphi(z,\tau)]. \tag{3.6}$$

At this stage, we obtain a possibility to describe spatial distributions of both the amplitude and the frequency chirp in the field $A(z,\tau)$. Because $q(z,\tau=\kappa z)\equiv 1$, spatial distribution for the peak amplitude $A_P(z)=A(z,\tau=kz)$ of guiding-center soliton of the first order ($\eta=1$) is determined by the modulus of Eq. (3.6)

$$A_P(z)=a_0\exp(-\Gamma z)\sqrt{1+R_0^2(z)} \tag{3.7}$$

The phase term in Eq. (3.6) makes it possible to find spatial distribution for the frequency chirp $b(z)$ of the same guiding-center soliton. The phase $\varphi(z,\tau)$ of fundamental soliton has no effect on the frequency chirp, so

$$b(z)=\left(\frac{\mathrm{d}^2}{\mathrm{d}\tau^2}\left\{\mathrm{arctg}\left[R_0(z)q^2(z,\tau)\right]\right\}\right)_{\tau=\kappa z}=\frac{-2R_0(z)}{1+R_0^2(z)}. \tag{3.8}$$

Each of Eqs. (3.7) and (3.8) includes three parameters: a_0, Γ, and Z_A, which are not independent from one another. Figs. 2a and 2b show spatial distributions for the peak

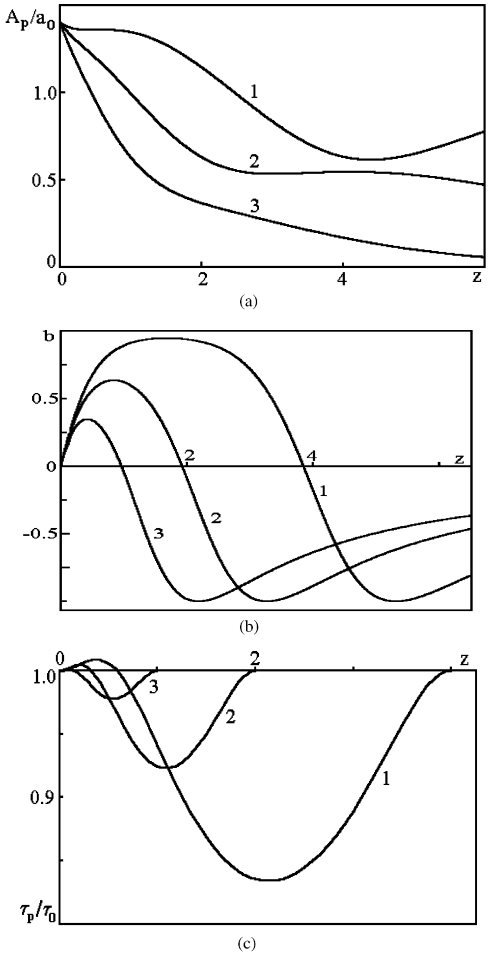

Fig. 2. Spatial distributions for the normalized peak amplitude (a), frequency chirp (b), and normalized pulse width (c) of guiding-center solitons with $a_0 = 1.4$: lines 1 are for $\Gamma = 0.2$; lines 2 are for $\Gamma = 0.4$, and lines 3 are for $\Gamma = 0.8$.

amplitude $A_P(z)$ and the frequency chirp $b(z)$ with $a_0 = 1.4$ and a set of Γ, corresponding to various Z_A.

To estimate spatial distribution for the pulse width of guiding-center solitons of the first order we apply the method of the phase plane. For this purpose the project of solution in the form of $A(z,\tau) = H(z,\tau)\exp[\mathrm{i} = \Theta(z,\tau)]$ can be substituted into Eq. (3.1), where $\Theta(z,\tau)$ is the complete phase of a guiding-center soliton in Eq. (3.6). Extracting the real part of the appeared equation and using approximation of the order of $0\left(R_0^4\right)$, we obtain

$$\frac{1}{2}\left(\frac{\partial H}{\partial \tau}\right)^2 + \Pi(H,z) = 0, \tag{3.9a}$$

$$\Pi(H,z) = -\frac{\eta^2 H^2}{2} + a_0^{-2}\exp(2\Gamma z)\frac{H^4}{2} - a_0^{-4}R_0^2(z)\exp(4\Gamma z)\left(\frac{2H^6}{3} - \frac{H^8}{2}\right) \tag{3.9b}$$

Here, Eq. (3.9b) describes the potential function $\Pi(H,z)$ for some particle with the mass of unity. Spatial distribution for the pulse width $T(\xi,z)$ at some pre-assigned level ξ of the amplitude function $H(z,\tau)$ is determined by the following integral relation

$$T(\xi,z) = \int_{\xi A_P(z)}^{A_P(z)} \frac{\mathrm{d}H}{\sqrt{-2\Pi(H,z)}}. \tag{3.10}$$

The function $A_P(z)$, see Eq. (3.7), determines the line, corresponding to maxima of pulse amplitudes and satisfying the condition $\Pi(A_0,z) = 0$. Selecting $\xi \approx 0.65$ in Eq. (3.10), one can obtain $T(0.65,z) \equiv 1/\eta$. Spatial distributions for the width of guiding-center solitons are shown in Fig. 2c. Eq. (3.10) makes possible describing, with accuracy of the order of $R_0^2(z)$, the primal property of guiding-center solitons of the first order to recover the width τ_p to its initial value τ_0 on passing through the distance $L_{\min}$ of peak compression to the return distance L_R [5–7]. It is seen from Fig. 1, that the area of applicability for the used approximations is restricted by some function $F(a_0,\Gamma,z)$ [8,9].

Such a solution can be compared with bright fundamental solitons adiabatically perturbed by low losses. An approximate expression for the complex amplitude of this solitary pulse is given by [3,11]

$$A(z,\tau) = a_P\exp(-2\Gamma z)\,\mathrm{sech}\left[\frac{\tau}{\tau_0}\exp(-2\Gamma z)\right] \times \exp\left\{-\mathrm{i}\Gamma\tau^2 + \frac{\mathrm{i}}{8\Gamma}[\exp(-4\Gamma z) - 1]\right\}. \tag{3.11}$$

Eq. (3.11) presents an approximate analytical description for evolutions of the peak amplitude, the pulse width, and the frequency chirp inherent in fundamental soliton, adiabatically perturbed by low losses in a fiber. Evolutions of the peak amplitude $A_P = a_P\exp(-2\Gamma z)$ and the pulse width $\tau_P = \tau_0\exp(2\Gamma z)$ follow from Eq. (3.11). An are of the applicability for Eq. (3.11) can be determined by

$$\tau^2 < \frac{\exp(-4\Gamma z)}{4\Gamma^2}. \tag{3.12}$$

When $\Gamma z \ll 1$, the exponent may be estimated as unity in Eq. (3.12), so we arrive at inequality $|\tau| < (2\Gamma)^{-1}$. Thus, Eq. (3.11) describes adequately the behavior of a solution to Eq. (3.1) in some temporal range being symmetrical relative to the center of a pulse. The magnitude of this range is in inverse-proportion to Γ with $\Gamma z \ll 1$. As pulse is passing, the effect of spatial coordinate dependence increases in Eq. (3.12) and the temporal range becomes to be narrower. Therefore, the smaller is the parameter Γ, the greater spatial-temporal range allows the solution obtained. For instance, in temporal range $-5 \le \tau \le 5$, containing the main part of energy for a sech-like optical pulse, one can obtain the restriction $\Gamma < 0.1$.

4. The advantages in applying guiding-center solitons as sync-signal carriers

Usually, the guiding-center solitons are associated with transmitting the digital data [3,7]. This paragraph is connected with the application of guiding-center solitons to the problem of creating lengthy fiber networks for a precise synchronization. Evidently, the preference should be given to the sync-signal carriers in the form of picosecond solitons being capable of passing through single-mode low-loss fibers at a short repetition period. The phenomenon of the self-phase modulation is capable of compensating a dispersive broadening of ultrashort pulse in the anomalous dispersion region of single-mode fiber and thereby of shaping a stable carrier in the form of "bright" picosecond optical soliton. Unfortunately, as it was mentioned above, the evolution of optical soliton in a fiber is also conditioned by the optical losses whose action is defined by the factor Γ, which represents the ratio of the dispersion distance Z_D to the loss distance γ^{-1}. If the factor $\Gamma = 0$, the initial balance between dispersion and nonlinearity gives rise to the fundamental soliton when the initial energy of such a pulse is $E_f = 2k_2(\sigma\tau_0)^{-1}$, where $\sigma = 2.7\,\mathrm{rad/W/km}$ in standard single-mode silica fiber. When $\Gamma \ll 1$, a fundamental soliton cannot exist in an ideal sense, because the optical losses induce adiabatical perturbation due to broadening on the soliton pulse as $\tau(x) = \tau_0 \exp(2\gamma x)$, see Eq. (3.11). In the case of $\Gamma \leq 1$ or $\Gamma > 1$, to realize the soliton-like regime of pulse propagation in a lossy fiber the initial energy of a pulse should be made larger than the energy of a fundamental soliton in the same but lossless fiber. Thus, we arrive at an opportunity to apply optical guiding-center solitons in a fiber that can be lengthy and lossy, to data processing as ultrashort carriers of information, in particular, as sync-signal carriers for precise synchronization. The initial energy of optical guiding-center soliton is $E_g = a_0^2 E_f$, where a_0^2 describes the above-mentioned excess of the optical pulse energy over the energy of an ideal fundamental soliton with the same initial width τ_0. During its propagation, the guiding-center soliton exhibits self-compression up to the propagation distance L_{min} and return of its own width to the initial value τ_0 followed by broadening a pulse, see Fig. 2c.

From the viewpoint of achieving the maximal accuracy of synchronization, associated with the minimal magnitude of the width τ_S of sync-pulse arriving at the point if indication, the potential designer of fiber network has two scopes for doing. The first scope is in using adiabatically perturbed fundamental soliton [3] whose initial width is determined as $\tau_0 = \tau_S \exp(-2\gamma L_0)$, where L_0 is the arm length. The second one is in exploiting the guiding-center soliton with $\tau_0 = \tau_S$ as a sync-signal carrier. The relation between the initial energies E_f and E_g is the governing factor in deciding between adiabatically perturbed fundamental soliton and guiding-center soliton whose width are the same at the distance associated with the arm length L_0, see Fig. 3.

The guiding-center soliton is initially less energetic than fundamental soliton, i.e. $E_g < E_f$, when the condition $L_0 > L_A = \gamma^{-1} \ln a_0$ is true. For typical magnitudes $a_0 = 1.4$ and $\gamma = 0.5\,\mathrm{dB/km}$ one can obtain $L_A = 5.84\,\mathrm{km}$. In this case $L_0 = L_R = 18.3\,\mathrm{km}$, and the potential designer can use either the adiabatically perturbed fundamental soliton with the initial width $\tau_1(x = 0) = 1\,\mathrm{ps}$ and the initial energy $E_f = 1.42\,\mathrm{pJ}$ or the guiding-center soliton with $\tau_2(x = 0) = 8\,\mathrm{ps}$ and $E_g = 0.34\,\mathrm{pJ}$ to obtain the same sync-pulse with $\tau_S = 8\,\mathrm{ps}$ at the point of indication, that leads to the accuracy of synchronization at the range of 16 ps. As this takes place, the initial energy of a sync-pulse in the guiding-center soliton regime turns out to be more than four times less than the energy of a sync-pulse using the adiabatically perturbed fundamental soliton regime. Then, the initial width of guiding center soliton is eight times more than the same value of adiabatically perturbed fundamental soliton. By this is meant that sync-pulses in the form of guiding-center solitons can be shaped easily with one and the same accuracy of synchronization. Thus, the guiding-center soliton is both energetically and technologically the best-suited sync-signal carrier for a fiber network under consideration. Consequently, we may conclude that the exploitation of guiding-center solitons as sync-pulses has an advantage in creating a medium-base fiber networks for a precise synchronization. Technically well-grounded parameters of both the sync-signal carrier and the single-mode fiber arm can be chosen using spatial dependencies of the amplitude and width for guiding-center solitons, presented in Fig. 2. It is clearly seen from Fig. 2a and c, that the primary self-compression stage is accompanied by the increase in the amplitude only when the factor Γ is small. In the other cases the monotonous lowering of the amplitude is observed. It follows from Eq. (3.6) that spatial–temporal distribution for the

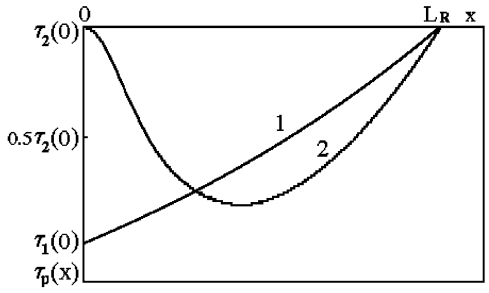

Fig. 3. The peculiarities inherent in developing the width for two types of soliton-like pulses of the first order as the carriers of sync-signals: line 1 is for the picosecond fundamental soliton adiabatically perturbed by low optical losses; line 2 is for the guiding-center soliton.

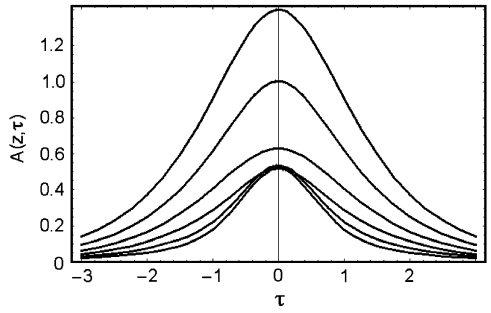

Fig. 4. Spatio-temporal distribution for the amplitude of guiding-center soliton with $a_0 = 1.4$ and $\Gamma = 0.4$; the set of curves correspond to the sequence: $z = 0,1,2,3,4$, and 5 in order of decreasing the pulse amplitude.

amplitude of guiding-center soliton can be expressed as

$$A_0(z,\tau) = a_0 \exp(-\Gamma z)\,\mathrm{sec\,h}(\tau) \times \left[1 + R_0^2(z)\,\mathrm{sec\,h}^4(\tau)\right]^{1/2}. \quad (4.1)$$

Fig. 4 shows additionally that both the maximum in amplitude distribution and the spatial-temporal shape of envelope for a guiding-center soliton sync-pulse, whose parameters $a_0 = 1.4$ and $\Gamma = 0.4$ are taken for example, has no any temporal shift while a pulse is passing through fiber arm. This fact demonstrates pictorially the possibility of exploiting picosecond optical guiding-center solitons as the carriers of sync-signals.

5. Technique of measuring the train-average clock skew

There are two groups of effects restricting the accuracy of interferometric technique on measuring the train-average clock skew between two soliton trains in fiber channels of the sync-network. The first group, including the amplitude and phase noise of pulse source together with the frequency chirp of an individual soliton pulse, is conditioned by intrinsic properties of interferometrically measured correlation function. The second group contains such factors as the noise of photodetector, number of samples, etc., appearing due to the processes of sampling and measuring. Let us briefly consider both the groups of effects starting from the first one. The amplitude noise is able to reduce the accuracy of determining the temporal parameters for individual pulses via processing the cross-correlation function obtained from the interference of a pair of single pulses, because this error depends on the ratio of the isolated pulse energy to the variance of random amplitude fluctuations. Optical sampling procedure of forming the correlation function, shaped by uninterrupted train of picosecond pulses, makes it possible to fulfill the train-average measurements with a desired accuracy, because large fluctuations are excluded. The phase noise has effect on the contrast of interferograms. This effect depends on the current time-delay in sliding interferometer, so when the time-delay is equal to zero or, what is the same – the instance of overlapping totally the corresponding individual optical pulses with each other, associated with the center of interferogram, any influence of the phase noise is absent. Thus, the effect of phase fluctuations on measuring the energetic center of interferometrically detected cross-correlation function is reduced to a minimum.

A combined output signal of sliding interferometer is proportional to the energy arriving at a photo-detector, if only the time of integration far exceeds the pulse width. Consequently, the second-order field strength correlation function, separated from a combined output signal, is given by

$$I(\tau) = \eta \int_{-\infty}^{+\infty} \left|E(t+\tau) + E(t)\right|^2 \mathrm{d}t, \quad (5.1)$$

where η is the factor, reflecting the properties of a photodetector whose time response may be, in its own turn, much greater than the pulse width; $E(t)$ is the optical field strength. The correlation function of a continuous wave radiation with the Gaussian statistics of amplitude fluctuations has the form

$$I(\tau) = 2\eta\sqrt{\pi}\tau_{\mathrm{C}}\left[1 + \exp\left(\frac{-\tau^2}{4\tau_{\mathrm{C}}^2}\right)\cdot\cos(\omega_0\tau)\right], \quad (5.2)$$

where τ_{C} is the interval of time coherence; here $\tau_{\mathrm{C}} = \tau_{\mathrm{AC}}/\sqrt{2}$, in this case the correlation function width τ_{AC} is determined at the amplitude level of $1/\sqrt{e}$ relative to a maximum of $I(\tau)$ in Eq. (5.2). Soliton-like optical pulse in a fiber has the given sech-like shape of envelope and it can be described as

$$E(t) = \mathrm{sech}\left(\frac{t}{\tau_p}\right)\cdot\exp[\mathrm{i}\varphi(t)]\cdot\exp(-\mathrm{i}\omega_0 t),\cdot \quad (5.3)$$

where ω_0 is the optical carrier frequency; τ_p is the pulse width at the amplitude level of $\mathrm{sech}(1) = 0.65$; $\varphi(t) = 0.5\,Q(t/\tau_p)^2$, here $Q = \mathrm{const}$ is the factor of linear frequency chirp. Substituting Eq. (5.3) into Eq. (5.1), one can obtain the following approximated result:

$$I(\tau) = 4\tau_{\mathrm{p}}\eta\left\{1 + \left(\frac{\tau}{\tau_P}\sqrt{1+Q^2}\right) \times\left[\mathrm{sh}\left(\frac{\tau}{\tau_p}\sqrt{1+Q^2}\right)\right]^{-1}\cos(\omega_0\tau)\right\}. \quad (5.4)$$

The estimation of Eq. (5.4) shows that the proper pulse width of a sech-like pulse and the width τ_A of its correlation function are approximately related as

$$\tau_p \approx 2^{-3/4}\sqrt{1+Q^2}\tau_A, \quad (5.5)$$

where τ_A is determined at the amplitude level of 0.65 relative to a maximum of $I(\tau)$ in Eq. (5.4). It is clearly seen from Eq. (5.4) that the presence of a linear chirp, i.e. $Q \neq 0$, does not deform a symmetry of the shape of interferome-

trically measured correlation function envelope, consequently the linear frequency chirp has no effect on the accuracy of calculating the energetic center of the field strength correlation function. Going to the correlation function for two pulse trains, we yield the same, but a train-average picture, which looks rather suitable.

The second group of effects restricting the accuracy of estimating the clock skew is associated with the processes of sampling and measuring. In sampling, an interferometrically designed field strength correlation function is represented by a sequence of samples taken at equal time intervals, so a desired accuracy of such a representation can be achieved only if the sampling frequency will be high enough. In particular, to recover an original optical signal, corresponding to all-optically shaped correlation function uniquely, the minimal sampling frequency should be not less than twiced maximal frequency inherent in the spectrum of that original signal. The procedure of discrete sampling makes it possible to come from problematical handing of the light frequencies to the operation with relatively low radio-frequencies, being suitable to conventional electronic processing. The registered electronic signal fits the optical correlation function in question adequately under certain conditions of detection. Usually, building a sinusoidal time-delay into one of its arms brings about the sliding in Michelson interferometer. The time-delay τ is varied with arm length due to the displacement $x(t)$ of sliding element as

$$\tau = c^{-1}x(t) \quad x(t) = x_0 \sin(2\pi ft) \tag{5.6}$$

where x_0 and f are the amplitude and frequency of sliding, respectively. The correlation function in question should be well precisely within the linear segment of a sinusoid: $\sin(2\pi ft) \approx 2\pi ft$. Suggesting that $|2\pi ft| \leq \alpha_0$, let us introduce the relative error $\delta = \alpha_0^{-1}(\alpha_0 - \sin\alpha_0)$, which determines a peak-to-peak displacement inside this linear segment as $x_L = 2x_0 \sin\alpha_0$. For instance, one can put $\delta = 0.045$, that is better than 5% in accuracy, hence $\alpha_0 = \pi/6$ and $x_L = x_0$. The twiced full spatial length $4C\tau_P$ of optical pulse should be therewith less than x_L, restricting the minimal magnitude of the amplitude of spatial sliding as $(x_0)_{\min} > 2C\tau_P/\sin\alpha_0$. However, each period of sliding includes two linear segments rather than one. This fact leads to shaping two secularly symmetrical correlation functions on photo-detector, one of which is practically useless. That is why the possibility exists of considering the only correlation function with increasing the time-delay, and to do this let us approximate the unidirectional sinusoidal displacement of sliding element within the linear segment in the following locally equivalent saw tooth form

$$x(t) = \frac{2x_m}{\pi}\sum_{n=1}^{\infty}\frac{(-1)^{n+1}}{n}\sin(2\pi nft). \tag{5.7}$$

The maximal amplitude x_m of equivalent saw tooth sliding can be estimated from a simple proportion: $(x_L/2\alpha_0) = (x_m/\pi)$ as $x_m \approx \pi x_0$, because the time derivative of Eq. (5.7) is constant and positive within the segment $(-\pi; +\pi)$. The frequency of sliding can be expressed as $f \approx V/(2\pi x_0)$, where V is the velocity of linear sliding. To reconstruct the proper correlation function without the loss in accuracy so-called noise of time quantization has to be taken into account, so the number m of photo-samples over one half-period of a light wave, i.e. over $\lambda_0/2$, should be chosen as: $m > \left[1 + (S/N)^2\right]^{1/2}$, where S/N is the signal-to-noise ratio. In practice, an intrinsic noise of optical signal is much less than the noise in electronic detection system whose level essentially governs the resulting ratio S/N. Nevertheless, the noise in detection system allows us to display the optical correlation function with a desired accuracy, corresponding to the given magnitude of the ratio S/N, such that $S/N \gg 1$ and there is the reason to put $m \geqslant (S/N)$. Since each photo-sample is connected with the arrival of an individual pair of optical pulses at photodetector, the number m can be determined as the ratio between the time of sliding the path $\lambda_0/2$ and the repetition period of optical pulses: $m = \lambda_0 f_R/(2V)$, where f_R is the repetition frequency of optical pulses. As a result, one can find an upper limit f_B on the frequency of sliding

$$f_B = \frac{\lambda_0 f_R}{4\pi x_0}\left(\frac{S}{N}\right)^{-1}. \tag{5.8}$$

Thus, when $f \leq f_B$, the inequality $m \geq (S/N)$ is true. During the process of measuring all-optically shaped correlation functions, see Eqs. (5.2) and (5.4), their electronic representations have the radio-wave carrier frequency f_E instead of the optical one $(2\pi)^{-1}\omega_0$. At any magnitude of f_E, the photo-detector time response should be sufficiently fast, i.e. its bandwidth should be rather wide to include f_E in order for such measurements to be made in their true values. To determine the magnitude of f_E we take into consideration that smooth electronic representation is actually some envelope for a lot of maxima (and minima) inherent in a radio-wave pulse with carrier frequency f_E. In such a picture, each following maximum is derived every time the path difference between the arms of sliding interferometer is varied over λ_0. Expressing the velocity V of sliding in units of λ_0 per second, we arrive at the relation: $f_E = V/\lambda_0$, so the time scale for electronic representation depends on the velocity V. To compensate this effect and to estimate the true time parameters of an original correlation function the time scale coefficient has to be introduced as $k_T = (2\pi f_E)^{-1}\omega_0 = (2\pi x_0 f)^{-1}c$. As this takes place, there is good reason to believe that the electronic representation is directly proportional to the optical correlation function with the time scale coefficient k_T, and consequently, it fits this function adequately with a desired accuracy. Finally, we consider the case, when an additional time-delay $\pm\Delta\tau$, i.e. in fact the clock skew t_C, see Eq. (2.3), is inserted into one of the interferometer's

arms, using aforementioned time-delay under control. The above-chosen approximation for the unidirectional displacement, see Eq. (5.7), with a positive time derivative leads to the following form of the second-order field strength correlation function

$$I(\tau \pm \Delta\tau) = \eta \int_{-\infty}^{+\infty} \left| E(t \pm \Delta\tau) + E(t+\tau) \right|^2 \mathrm{d}t, \qquad (5.9)$$

which is shifted in time for the value of $\Delta\tau$ relative to the starting position with $\Delta\tau = 0$ instead of Eq. (5.1). The magnitude of $\Delta\tau$ is limited by the inequality $2c\Delta\tau \leq x_L$, i.e. by the boundaries of linear sliding. Naturally, the electronic representation of this correlation function, scaled in time, is also shifted, but for the value of electronically displayed clock skew $\Delta\tau_E$, which has the form: $\pm\Delta\tau_E = \pm\Delta\tau \cdot k_T$. The sign of electronically displayed clock skew is uniquely determined by the corresponding sign of initially introduced time-delay due to Eq. (5.7). These combined things give a possibility of measuring interferometrically the train-average clock skew.

6. Schematic arrangement and experimental results

The following all-optical scheme, being the key part of sync-network under consideration, has been extracted and experimentally simulated on a mock-up, see Fig. 5. The source of the lock-on signals generates uninterrupted train of identical powerful picosecond pulses at the wavelength λ_S. Taken alone, an individual pulse from that train is transmitted by optical isolator and then is divided by a 3-dB Y-coupler in two equal portions each of them passes at the input plug of corresponding fiber channel. Initially, each partial pulse, owing to its own parameters, is capable of shaping the fundamental guiding-center optical soliton in a fiber of either transmitting channel, on subtraction of losses due to their distribution. Just this picosecond optical soliton represents the lock-on signal, propagating to the observing post with the opto-electronic converter for received data signals, then being effectively reflected by spectrally selective mirror, coming back in soliton regime and, finally, arriving at one of two input ports of sliding Michelson interferometer, upon the second distribution by the wave division demultiplexer and spectrally insensible Y-coupler associated with the corresponding channel. A sinusoidal time-delay is built into one of the arms of sliding interferometer, see Fig. 6, whose other arm is equipped by two time-delay lines, which are not shown. One of these delay lines is manually controlled with the accuracy down to ± 0.05 ps to calibrate the mock-up, whereas the other one is controlled electronically to simulate the action of external perturbations. As a result, the sliding interferometer detects the train-average clock skew following

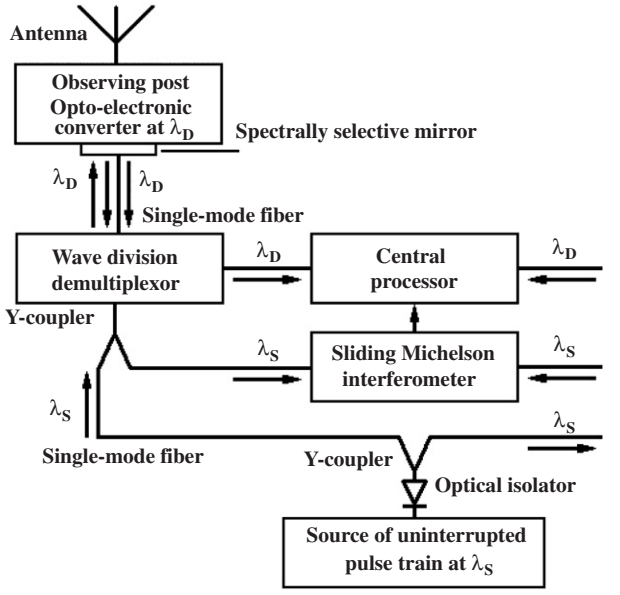

Fig. 5. Schematic arrangement of an all-optical sync-network (one of two arms is shown).

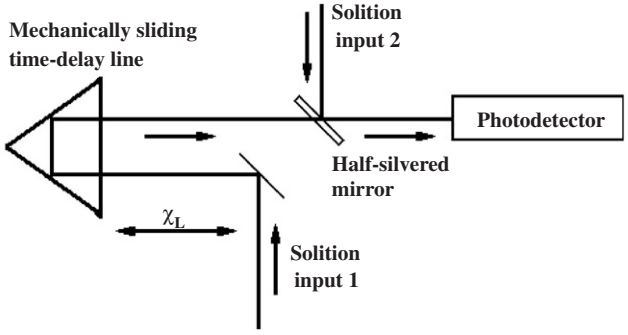

Fig. 6. Optical scheme of the sliding Michelson interferometer under consideration (all the additional time-delay lines are excluded).

which the local processor calculates its value. Opto-electronic converters transform electronic data signals from antennas to optical data signals at the carrier wavelength λ_D. Spectrally selective mirrors in either channel have both the reflectivity at the wavelength λ_S and the transmissivity at the wavelength λ_D enlarged to a maximum, so the sync-pulses are reflected without destroying an adiabatically perturbed soliton regime of their propagation and, in their own turn, all the optical data signals pass into fiber channels through these mirrors with little or no changes. The optical isolator keeps therewith a cavity of pulse generator from the passage of the reflected sync-pulses. Consequently, the optical data signals have the only way at the input ports of the central processor, which determines true values of data taking into account repeatedly calculated train-average clock skew.

During the experiment the picosecond optical soliton sync-pulses are shaped in single-mode fiber arms by

semiconductor laser source based on single-mode InGaAsP-heterostructure with an external fiber cavity, operating in the active mode-locking regime on the wavelength of 1320 or 1550 nm [13,14]. In the beginning, the time coherence for semiconductor lasers has been estimated in a continuous wave regime of radiation when the auto-correlation function has a smooth envelope, see Eq. (5.2). Experimentally obtained auto-correlation trace with $\tau_{AC} \approx 15$ ps, corresponding to this case, gives a possibility to estimate the interval τ_C of time coherence, which comprised about 10 ps for heterostructures as were used. In the regime of active mode-locking, these semiconductor lasers generate slightly chirped, but soliton-in-fiber deriving pulses, whose width lies in the range from 2 to 4 ps and repetition frequency can be varied between 400 and 1150 MHz. Applying the formulae, listed in Section 5, the following set of performances for sliding may be selected with major reserve for experimental realization: $\delta = 0.045, x_0 = x_L = 30$ mm, $f = 1$ Hz, and $(S/N) = 10$ to provide the range of temporal sliding up to 100 ps, resulting in $k_T = 1.6 \times 10^9$. The calibration of this mock-up lies in locating the starting position with the help of manually controlled time-delay line. The fineness of control over the length in each fiber arm is accurate to better than 0.01 mm, corresponding to the time interval of 0.05 ps in silica fiber. The last value does not have effect on the accuracy of measuring the train-average clock skew, because it is much less than the interval of time coherence. The temporal range of measuring the train-average clock skew t_C is determined by the complete path length x_L of linear sliding. When uninterrupted trains of optical soliton lock-on signals are applied at either input of sliding Michelson interferometer, the cross-correlation function trace is registered at the center of scale, i.e. at the starting position, for lack of any external perturbations in the calibrated scheme, see Fig. 7a. The repetition period of displaying such a trace is determined by the magnitude of f restricting, among other things, permissible characteristic times of varying any external perturbations, which may be tolerated via interferometric correlation technique of measurements using the procedure of sampling. In order for trial experiments with the optical scheme calibrated in advance, an additional time-delay $\Delta\tau$ has been brought in one of the transmitting fiber channels with the help of electronically controlled time-delay line to simulate the action of external perturbations. When the magnitude of $\Delta\tau$ is varied, in particular occasionally, the cross-correlation function trace becomes shifted across the time scale relative to the starting position as it is shown in Fig. 7b and c. It is clearly seen that the amplitude, width and shape of envelope as well of the cross-correlation function trace, on shifting, remain unchanged. We have defined that the measured values of the train-average clock skew t_C exhibit an accuracy of $\pm$ 0.1 ps, when the total magnitude of linear sliding lies in the temporal range of $\pm$ 50 ps, so the resolution up to 500 points has been achieved.

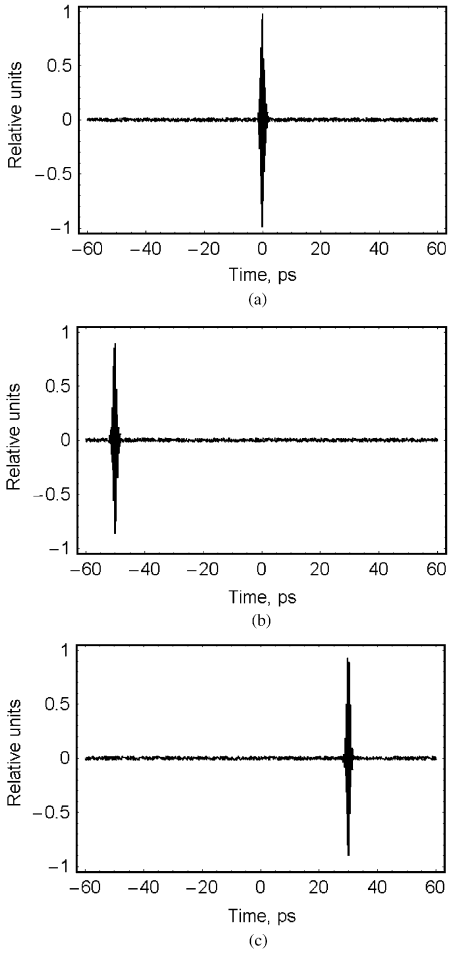

Fig. 7. The digitized oscilloscope traces of the cross-correlation functions: (a) at the center of the calibrated scale, (b) shifted by $t_C \approx -50$ ps, and (c) shifted by $t_C \approx +30$ ps from the center.

7. Conclusion

The distribution of lock-on signals can be arranged using the spatial optical interconnections as well as the index-guiding structures. On the one hand, the spatial interconnections may be made with the help of focusing or defocusing design. The spatially defocused interconnections have rather low efficiency, because only a small part of light arrives at photodetectors. At the same time, the necessity of both collimating the light into focal spots as small as the wavelength of light and aligning strongly this pattern is the main disadvantage for the spatially focused interconnections. On the other hand, the index-guiding structures can be based on the integrated optic waveguides or on the optical fibers. The difficulty of applying the integrated optic waveguides is conditioned by the complexity of constructing a long-haul and branched optical network as well as by their own properties, including insertion losses and optical damage. In particular, dispersion and losses inherent in a waveguide impede the passage and distribution of ultrashort

optical lock-on signals through a similar network. That is why, to pass the lock-on signals with the minimal duration and to distribute these signals all over the processing system the optical fiber technique is the most suitable. The use of ultrashort soliton pulses in fibers as the optical lock-on signals allow us to achieve a sub-picosecond accuracy of synchronization at the repetition rate up to 100 GHz and, consequently, to increase the informative capabilities of the processing system without any revisions in its architecture. Evidently, it does not make up any difficulties in distributing the optical soliton lock-on signals over the branched fiber sync-network. Moreover, it is rather reasonable to assume that semiconductor laser generator of uninterrupted train, including picosecond sync-pulses, is quite suitable just for optical fiber network.

To apply picosecond optical solitons to the problem of precise synchronization we have analyzed the model, described by the complex cubic Ginzburg–Landau equation in a reduced form, and presented approximate analytical description for the evolution of such main parameters as the amplitude, width, and frequency chirp for guiding-center solitons in optical fibers. Key physical aspects of implementing a novel all-optical synchronization technique, based on picosecond guiding-center solitons as the ultrashort optical carriers of sync-signals passing through silica long-haul single-mode fibers, have been briefly discussed. Our attempt to similar application has its origins in the two above theoretically established circumstances. First, the property of a guiding-center soliton to return of its own width to the initial value that can be put into operation to chose the fiber arm length, and second, the maximum in amplitude distribution of guiding-center soliton sync-pulse has no temporal shift while a pulse is passing through a fiber arm. Two types of soliton-like pulses, being potentially suitable to be the sync-signal carriers, have been compared with each other. The analysis of the relation between the initial energies of these pulses has shown that the guiding-center soliton has an advantage over the adiabatically perturbed fundamental soliton as the sync-signal carrier in a medium-base fiber network. Moreover, evidently the exploitation of guiding-center solitons will be technologically easily, because they are wider initially and that corresponding fundamental solitons can be generated easily.

The potentialities inherent in optical interferometric technique of measuring precisely time intervals with the help of the second-order field strength correlation functions averaged over a train have been analyzed. Such a technique has the advantage that it is capable of operating on low-power picosecond optical pulse trains, for example, picosecond guiding-center solitons in single-mode fibers, generated by semiconductor laser sources, to a sub-picosecond accuracy. The schematic arrangement of the soliton sync-network, oriented to the radio-interferometer with a high angular resolution and a short base, has been proposed. Some results of successfully fulfilled trial experiments with a specially designed mock-up for an optical part of similar soliton sync-network have been considered. In particular, observational data on transmitting the picosecond soliton lock-on signals and the evidence on processing the train-average clock skew have been presented.

Acknowledgments

Finally, the authors are grateful to I.S. Tarasov for powerful single-mode InGaAsP-semiconductor lasers put at our disposal for the purpose of trial experiments and to Yu.I Fedukovsky for the fruitful discussions. This work was financially supported by the CONACyT (Mexico), project 41998-F.

References

[1] A. Hasegawa, Y. Kodama, Guiding-center soliton in optical fibers, Opt. Lett. 15 (24) (1990) 1443–1445.
[2] A. Hasegawa, Y. Kodama, Guiding-center solitons, Phys. Rev. Lett. 66 (2) (1991) 161–164.
[3] A. Hasegawa, Y. Kodama, Solitons in Optical Communications, Clarendon Press, Oxford, 1995.
[4] K.J. Blow, N.J. Doran, Average soliton dynamics and the operation of soliton systems with lumped amplifiers, IEEE Photon. Technol. Lett. 3 (1991) 369–371.
[5] A.S. Shcherbakov, E.I. Andreeva, Observation of picosecond optical pulses with guiding-center soliton in a single-mode fiber-optic waveguide, Tech. Phys. Lett. 20 (11) (1994) 873–875.
[6] A.S. Shcherbakov, E.I. Andreeva, I.S. Tarasov, Experimental investigation of guiding-center solitons in optical fiber, Proc. SPIE 2800 (1995) 333–340.
[7] A.S. Shcherbakov, E.I. Andreeva, Performance data of lengthy span soliton transmission system, Opt. Fiber Technol. 2 (2) (1996) 127–133.
[8] A.S. Shcherbakov, A.Yu. Kosarsky. Shaping, propagation of the first-order guiding-center solitons inherent in solutions of the complex Ginzburg–Landau equation, Tech. Phys. Lett. 26 (7) (2000) 620–622.
[9] A.S. Shcherbakov, A.Yu. Kosarsky, E.E. Tepichin, Area of existing the first order guiding-center solitons of the complex cubic Landau-Ginzburg equation, Bull. RAS, Phys. 65 (6) (2001) 881–885.
[10] N.N. Akhmediev, A. Ankiewich, Solitons Nonlinear Pulses and Beams, Chapman & Hall, London, 1997.
[11] G.P. Agrawal, Nonlinear Fiber Optics, Academic Press, San Diego, 2001.
[12] J. Satsuma, N. Yajima, Initial value problems of one-dimensional self-modulation of nonlinear waves in dispersive media, Prog. Theor. Phys. Suppl. 55 (1974) 284–306.
[13] E.I. Andreeva, A.S. Shcherbakov, I.E. Berishev, Yu.V. Il'in, I.S. Tarasov, Semiconductor generator of binary words formed by picosecond optical pulses, Tech. Phys. Lett. 19 (9) (1993) 538–540.
[14] A.S. Shcherbakov, E.I. Andreeva, Semiconductor source of digital trains including soliton-like pulses, Bull. RAS, Phys. 58 (2) (1994) 154–157.